The Storage of Antecedent Precipitation and Air Temperature Signals in Soil Temperature over China

YAOMING SONG,[a,b] ANNING HUANG,[c] AND HAISHAN CHEN[a,b]

[a] Collaborative Innovation Center on Forecast and Evaluation of Meteorological Disasters/Key Laboratory of Meteorological Disaster, Ministry of Education, Nanjing University of Information Science and Technology, Nanjing, Jiangsu, China
[b] School of Atmospheric Sciences, Nanjing University of Information Science and Technology, Nanjing, Jiangsu, China
[c] CMA-NJU Joint Laboratory for Climate Prediction Studies, School of Atmospheric Sciences, Nanjing University, Nanjing, Jiangsu, China

(Manuscript received 11 June 2021, in final form 17 December 2021)

ABSTRACT: Soil temperature (ST) is one of the key variables in land–atmosphere interactions. The response of ST to atmospheric changes and subsequent influence of ST on atmosphere can be recognized as the processes of signals propagation. Understanding the storing and releasing of atmospheric signals in ST favors the improvement of climate prediction and weather forecast. However, the current understanding of the lagging response of ST to atmospheric changes is very insufficient. The analysis based on observation shows that both the storage of air temperature signals in deep ST even after 4 months and the storage of precipitation signals in shallow ST after 1 month are widespread phenomena in China. Air temperature signals at 2 m can propagate to the soil depths of 160 and 320 cm after 1 and 2 months, respectively. The storages of antecedent air temperature and precipitation signals in ST are slightly weaker and stronger during April–September, respectively, which is related to more precipitation during growing season. The precipitation signals in ST rapidly weaken after 2 months. Moreover, the effects of accumulated precipitation and air temperature on the signal storage in ST have significant monthly variations and vary linearly with soil depth and latitude. The storage of antecedent air temperature or precipitation signals in ST exhibits an obvious decadal variation with a period of more than 50 years, and it may result from the modulation of the global climate patterns which largely affect local air temperature and precipitation.

KEYWORDS: Atmosphere; Land surface; Atmosphere-land interaction; Soil temperature

1. Introduction

Soil temperature (ST) represents land surface energy status and heat storage, and it is a key state variable in land–atmosphere interaction. ST affects monthly to interannual climate variations by changing water and heat fluxes between land surface and atmosphere (Hu and Feng 2004a,b; Mahanama et al. 2008; Wu and Zhang 2014). ST facilitates convective development (Liu and Avissar 1999; Xue et al. 2018), leading to changes in locations and intensities of precipitation (Fan 2009), and plays an important role in the extreme heat events (Gómez et al. 2016).

The persistence of ST anomalies can affect the subsequent atmosphere. Tang et al. (1987) found that the precipitation in spring may be affected by the ST at the depth of 0.8 m in winter. Ma (1995) revealed some evidence of a connection between the serious floods in the Yangtze–Huaihe River basin and the antecedent ST anomalies at the depths of 1.6 and 3.2 m. Mahanama et al. (2008) showed that the summer precipitation has good correlation with the late spring ST. Xue et al. (2012) demonstrated the summer precipitation in North American is well related to the spring subsurface ST anomaly in the western United States.

The effect of ST on subsequent atmosphere depends on the persistence of ST anomalies, which is called ST memory. The memory of ST can persist for 1 month to years, depending on soil depth, season, and climate regime (Liu and Avissar 1999; Yang and Zhang 2016). The ST anomaly is the response to the atmosphere anomalies, and ST is affected by precipitation (García-Suárez and Butler 2006), radiation, air temperature (Kang et al. 2000; Zhang et al. 2001; Beltrami et al. 2005; Zhang et al. 2021), soil physical properties (Ceccon et al. 2011), vegetation cover types (Zhang and Li 2018; Hu et al. 2009; Tesař et al. 2008), wind speed (Mihalakakou et al. 1997), snow (Qian et al. 2011; Iijima et al. 2010), and topography changes (Wundram et al. 2010). Although ST is affected by various factors, precipitation and air temperature are two main factors (Helama et al. 2011; Yang et al. 2018). Zhang et al.(2021) demonstrated the effect of air temperature on ST can take up to 10 months to propagate downward to the depth of 320 cm. The ST at soil depth below 100 cm is highly correlated with air temperature (Chen et al. 2020).

There are two main processes in the complete process chain of the interactions between ST and atmosphere, the first one is that atmosphere anomalies lead to abnormal ST, and the second one is that abnormal ST affects atmosphere in turn. The study on the second process can improve the predictions of atmosphere through understanding the relationship between ST and subsequent atmosphere, and the study on the first process helps understand the processes of ST storing atmospheric

Supplemental information related to this paper is available at the Journals Online website: https://doi.org/10.1175/JHM-D-21-0126.s1.

Corresponding authors: Yaoming Song, songym@nuist.edu.cn; Anning Huang, anhuang@nju.edu.cn

DOI: 10.1175/JHM-D-21-0126.1

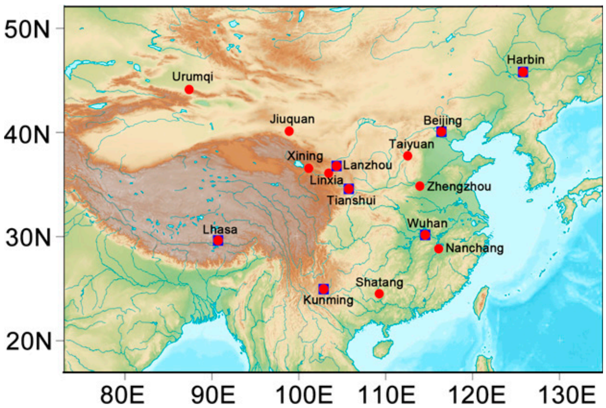

FIG. 1. The location of sites during 1960–2013; the blue boxes denote the sites for analyzing decadal variations of the relationships between ST and antecedent precipitation or air temperature.

anomalies. The systematic and overall understanding of these two processes is helpful to construct the relationship between the antecedent and subsequent atmospheric anomalies, which are of important significance to deepen the understanding of the complex interactions in the climate system and improve the lead time of atmospheric forecasting.

As the key variables reflecting the soil heat and water storage, ST and soil moisture are crucial in land–atmosphere interactions. However, most studies have focused on soil moisture with less attention to ST, and the understanding of the process of ST storing atmospheric anomalies is seriously insufficient. The following questions need to be further indicated: 1) For how long can ST store the atmospheric signals? 2) What are the differences among the ST storing antecedent atmospheric signals at different latitudes, different soil depths, and in different months? 3) How has ST storing atmospheric signals changed in recent decades? And what are the relevant impact factors? The main aim of this study is to deepen the understanding of the storage of atmosphere signals in land, which is one of the essential processes in land–atmosphere interactions in climate system. Because precipitation and air temperature are two main factors affecting ST (Helama et al. 2011; Yang et al. 2018), the atmospheric variables considered are air temperature and precipitation in this study.

2. Data and methods

a. Data

The observed monthly data in this study are provided by the China Meteorological Administration. The data include monthly precipitation, air temperature (1.5 m), and ST at the seven layers of 5, 10, 20, 40, 80, 160, and 320 cm during 1960–2013. Due to the large number of missing values in ST data, we adopted 15 sites with enough valid data at seven soil layers during 1960–2013, in which the data at 7 sites (Fig. 1) were used to analyze the time variation of the relationship between ST and antecedent air temperature or precipitation in recent decades. Moreover, we also used the 30-min interval data including precipitation, 2-m temperature, and ST observed at the Tongyu site (44°25′N, 122°52′E) in 2004 to analyze the frequency characteristics in air temperature, precipitation, and ST.

b. Methods

The storage of antecedent precipitation and air temperature signals in ST is affected by meteorological condition, land cover and soil texture, etc., and the common characteristics of the storage are studied to deepen macro understanding of the storage of atmosphere signals in ST over China. The storage of atmospheric signals in ST is described by the consistency of atmospheric and ST signals, which is depicted quantitatively by correlation coefficients. The lag correlation coefficient is used to analyze the relationships between ST and antecedent air temperature (R-ST-T) or precipitation (R-ST-P) (Fig. 2). First of all, the correlations are analyzed for the whole period of 1960–2013, reflecting the overall

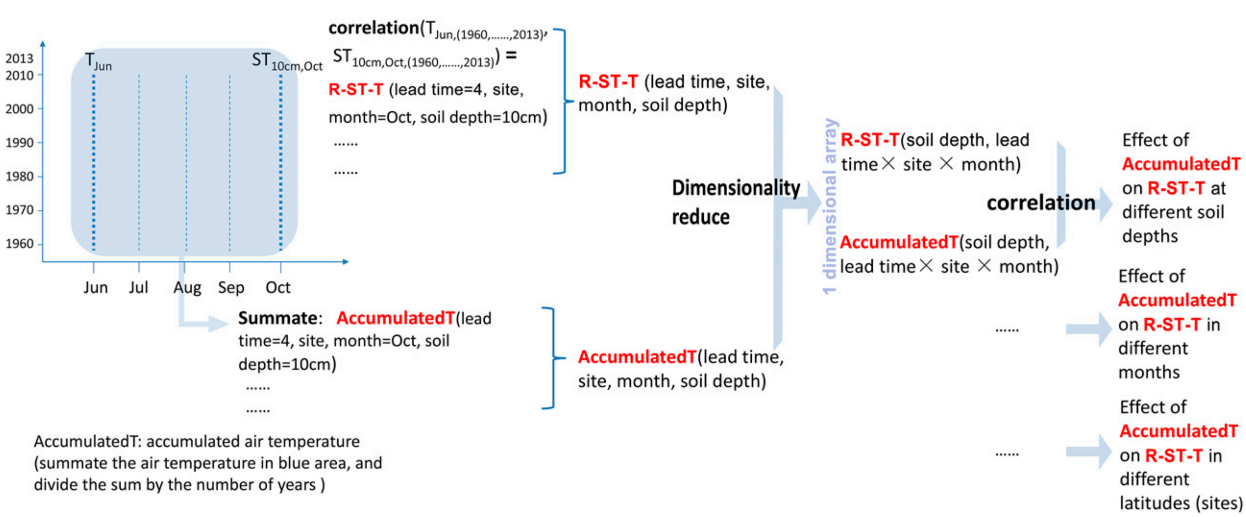

FIG. 2. Flowchart of calculating the R-ST-T and the effect of accumulated air temperature on the R-ST-T.

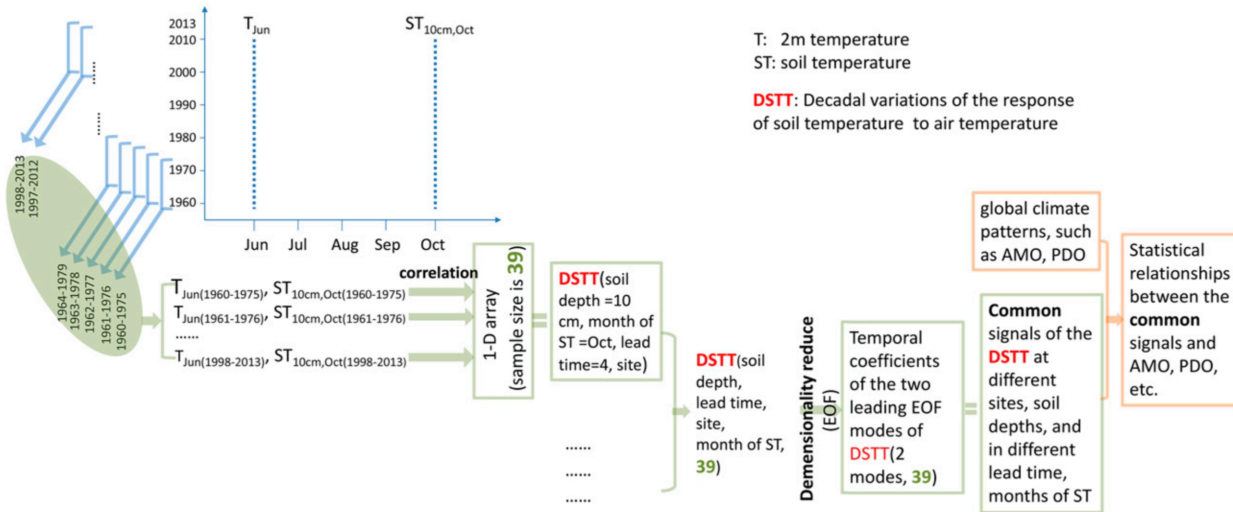

FIG. 3. Flowchart of calculating decadal variations of the response of ST to air temperature, and the relationships between the decadal variations and global climate patterns, such as AMO, PDO, AO, and IPO.

characteristics of R-ST-T and R-ST-P. Empirical orthogonal function (EOF) is used to decompose the correlations to get the characteristics of R-ST-T or R-ST-P at different soil depths with different lead times and the corresponding variations of the characteristics with months and sites, by extracting common signals of the correlations at different sites in different months. Second, the correlation coefficients between accumulated air temperature (precipitation) and R-ST-T (R-ST-P) are used to show the accumulated effect of atmosphere on the storage of antecedent atmospheric signals, and the changes of accumulated effect with latitude and soil depth are also studied. The accumulated precipitation (air temperature) is the sum of precipitation (air temperature) during the period between the lead time and the time of ST averaged over 1960–2013. For example, to get the effect of accumulated precipitation on the R-ST-T between air temperature in June and ST in October, the total precipitation from June to October is averaged over 1960 to 2013, and then we get an array with different lead times, months of ST, soil depths, and sites. For different months of ST, the array reduced the dimensionality to be one-dimensional data (sites × depths × lead times) and to do the same for the R-ST-T. The correlation between the two one-dimensional data is used to express the effect of accumulated precipitation (Fig. 2). Third, sliding correlation with a 16-yr window is used to study the decadal variations of the response of ST to antecedent atmospheric conditions. In this method, 39 sliding correlation coefficients between ST and antecedent air temperature or precipitation with the 16-yr window are calculated during 1960–2013. And then, we reduce the dimensionality of the 39 sliding correlation coefficients at each soil depth of each site in each month to two-dimensional data (sites × depths × months, 39), which is used to exact the common decadal variation signals of the above sliding correlation coefficients by EOF analysis (Fig. 3). Finally, composition analysis and correlation coefficient analysis are used to reveal the relationship between the common decadal signals and global climate patterns, and the influence of atmospheric condition on these relationships.

3. Results

a. Storage of antecedent precipitation and air temperature signals in ST

The previous studies show that the changes in antecedent precipitation and air temperature can cause the changes in ST, which also can be expressed as the propagation of abnormal signals. To describe the common features in the relationships between ST and antecedent air temperature or precipitation in different regions over China, the number of the sites with high correlations between ST and antecedent air temperature or precipitation at all 15 sites is used to reveal spatial distribution range of the high correlations in R-ST-T or R-ST-P over China. On the whole, there are obvious seasonal variations in the spatial distribution range of R-ST-P, especially at soil depths above 50 cm, while the seasonal variations are complex for R-ST-T (Fig. 4). Moreover, there are more sites with significant correlations in R-ST-T than in R-ST-P (Fig. 4). In R-ST-T and R-ST-P, the number of the sites with significant correlations (correlation coefficient between ST and antecedent air temperature or precipitation is significant if it is within 95% significance interval in section 3a) decreases obviously as the soil depth increases for the shorter lead time, and it is opposite for the longer lead time (Fig. 4), which means that the signals of antecedent precipitation or air temperature propagate to the deeper soil layers with time. The number of the sites with significant correlations decreases rapidly as the lead time increases in shallow soil layers, and the number of sites with significant correlations changes little in deep soil layers when the lead time is longer than one month. Significant

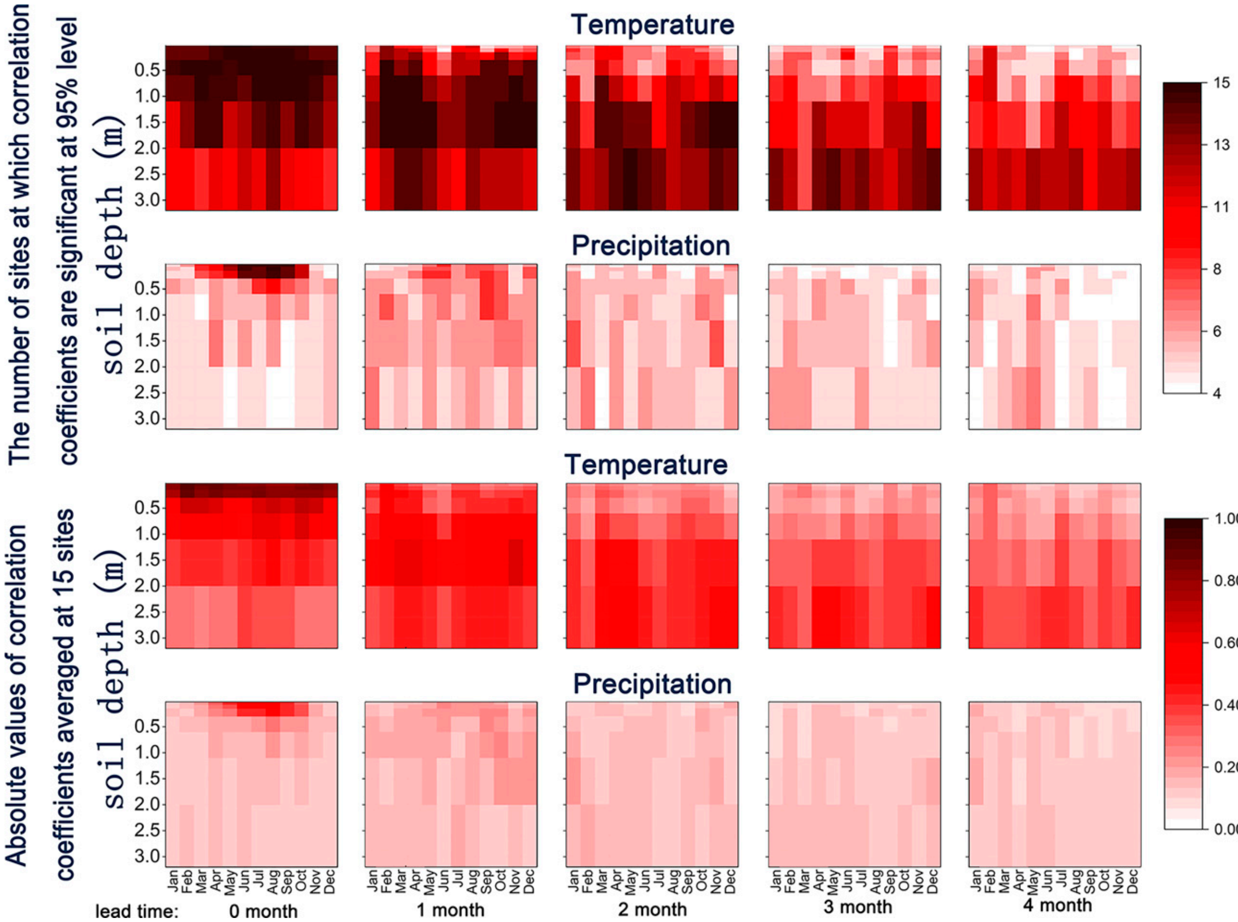

FIG. 4. The number of the sites at which the lag linear correlation coefficients between ST and antecedent temperature or precipitation are significant at the 95% and the absolute values of correlation coefficient averaged over the 15 sites at different lead times and at different soil depths.

correlations at most sites with the air temperature leading the ST by 1 month (2 months) are noted at the soil depth of 160 cm (320 cm) (Fig. 4). The correlations at the soil depths of 160 and 320 cm for about 10 sites out of the 15 sites are significant with a lead time of 4 months during most of the year. In one word, the storage of antecedent air temperature signals in deep ST even after 4 months is a common phenomenon in China.

The number of sites with significant correlations between ST and antecedent precipitation with the lead time of 0–1 month at the top 40-cm soil depth varies with time obviously, especially in the rainy season during which much larger number of sites is noted, while the number of sites with significant correlations between ST and antecedent precipitation with different lead times below the soil depth of 40 cm show much smaller differences among different months. It can be seen that more precipitation can propagate stronger signals into ST after about one month in the shallow soil at most sites (Fig. 4), and the signals of antecedent air temperature or precipitation can propagate to the deeper soil layers with time.

Meanwhile, it is noted that the absolute values of correlation coefficients averaged over the 15 sites display similar monthly variations to the number of sites with significant correlations (R-ST-P and R-ST-T), suggesting that the higher absolute values of the correlations are corresponding to the more sites with significant correlations.

It can be seen in Fig. 4 that the relationships between ST and antecedent precipitation or temperature are obviously different at different soil depths, so how do the relationships change with soil depth at different sites? Figure 5 shows that the ratio of correlation coefficients with 95% significance level relative to the total correlation coefficients between ST and antecedent air temperature at different soil depths and different sites is much higher than that between ST and antecedent precipitation regardless of the lead time and month, and the number of the total correlation coefficients is 60 (months × lead times). The percentage of significant correlations increases with soil depth, especially for the correlation between ST and antecedent air temperature. The percentage is higher at Lhasa, Kunming, and Lanzhou for antecedent air temperature, while the percentage is higher at Urumqi, Beijing, Lanzhou, Kunming, and Nanchang in the whole soil for antecedent precipitation. At the sites mentioned above, ST has a longer and stronger storage of antecedent air

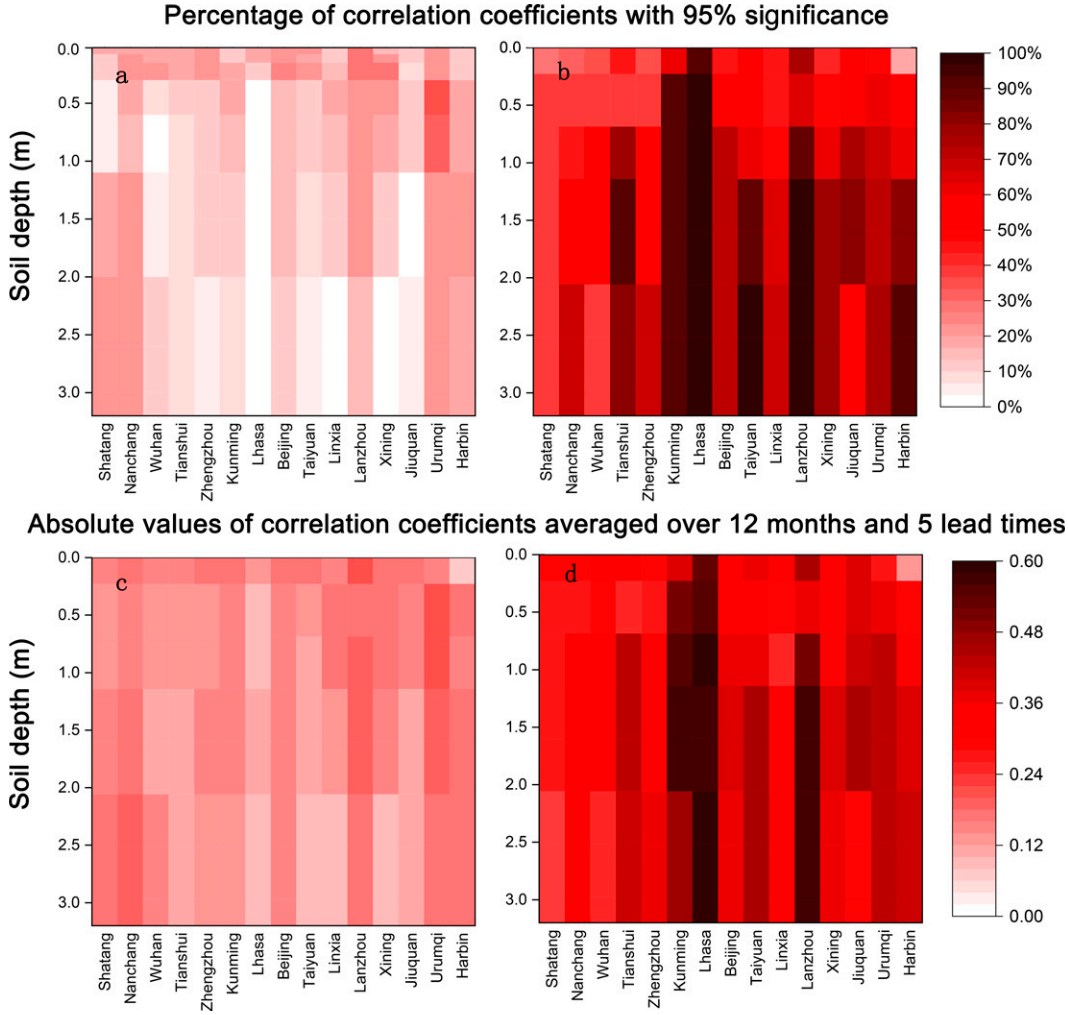

FIG. 5. The percentage of the number of correlation coefficients with 95% significance level relative to the total number of correlation coefficients across five lead times and 12 months, and absolute values of correlation coefficients averaged over 12 months of a year with five lead times at different soil depths and different sites. (a),(c) The correlation coefficients between ST and antecedent precipitation; (b),(d) the correlation coefficients between ST and antecedent air temperature.

temperature and precipitation signals. The composition analysis shows that the sites with higher (lower) R-ST-P and R-ST-T at a soil depth of 40 cm corresponding to the less (more) precipitation and lower (higher) air temperature, suggesting that the differences of the correlations at the above sites may be significantly affected by different climate conditions (Fig. S1 in the online supplemental material). Air temperature and precipitation can change ST by land–atmosphere interactions, and then interfere with the storage and propagation of antecedent precipitation or air temperature signals in ST. For example, more precipitation results in more soil water, which in turn has a larger impact on ST.

As shown in Fig. 4, the relationships between ST and antecedent precipitation or temperature are various at different lead times in different months, so how do the relationships vary with lead time at different sites? Figure 6 shows that the percentage of significant correlations between ST and antecedent air temperature is higher than that between ST and antecedent precipitation, and the number of the total correlation coefficients is 84 (months × soil depths). The percentages of significant correlations obviously decrease with lead time. For air temperature, the much higher percentages can be noted at Lhasa, Kunming, Taiyuan, Tianshui, and Lanzhou. For precipitation, the percentages at different sites show slightly differences, except for Urumqi and Nanchang, where the percentages are higher. It can be inferred from Figs. 5 and 6 that the significant correlations are mainly located in deep (shallow) soil for antecedent air temperature (precipitation), and the percentages decrease with lead time.

As shown in Fig. 7, the high correlations between ST and antecedent air temperature have an obvious tendency to shift to deep soil and gradually reduce as lead time increases, and

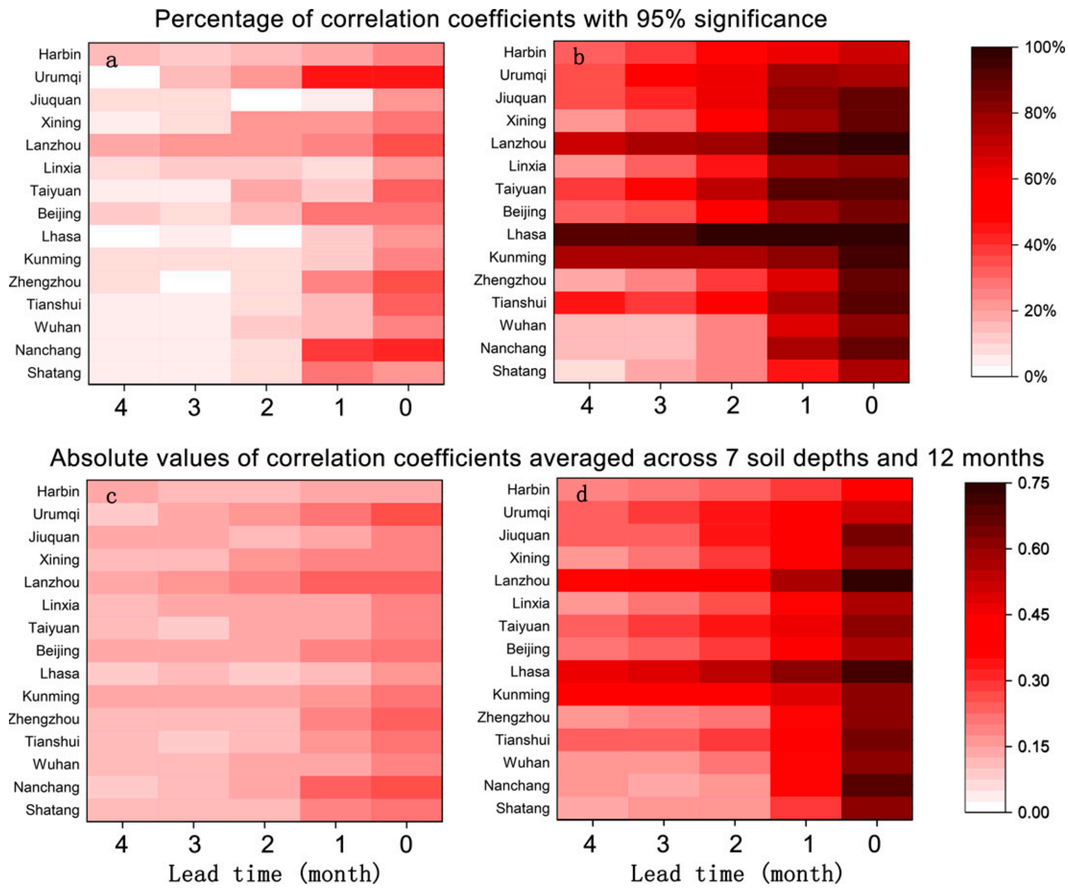

FIG. 6. As in Fig. 5, but for the percentage of the number of the correlation coefficients and absolute values of correlation coefficients averaged across 12 months and seven soil depths when the sites and lead times are changed.

this feature is more obvious at Kunming, Lhasa, Urumqi, Xining, and Harbin. The antecedent air temperature signals with the lead time of 1 and 2 months are the most obvious at the soil depths of 160 and 320 cm, respectively, or in other words, the antecedent air temperature signals can propagate to the soil depths of 160 and 320 cm after 1 and 2 months, respectively. Moreover, the correlations are slightly weak from April to September, which may be related to the interference from the much more rain during the growing season. In a word, the air temperature signals can propagate to the soil depths of 160 and 320 cm after 1 and 2 months, respectively, and the storage in ST is relative weaker during the growing season.

Figure 8a shows that the correlation coefficients between ST and antecedent precipitation decrease with lead time and soil depth for the first leading EOF mode, which can explain 46.2% of the total variance. There is a high correlation area in middle soil depths at the lead time of three months in the second leading EOF mode (Fig. 8c), which can explain 12.2% of the total variance. Moreover, there are significant monthly variations in the two leading EOF modes (Figs. 8b,d). Figures 8e–g show reconstructed correlation distributions at different soil depths based on the first and second leading EOF modes in January–March, April–October and November–December, respectively. There are obvious negative correlations between ST and antecedent precipitation, and the correlations are stronger in April–October than in January–March and November–December. In April–October, the correlations weaken with the increase of lead time and soil depth. At the soil depths of 0.6–2.7 m, the correlations are stronger with one month lead time than the ones with other lead times. Moreover, the correlations rapidly weaken at the lead time of 2 months (Fig. 8f). In January–March and November–December, the correlations with different soil depths and lead times have similar characteristics, and the antecedent precipitation signals spread in the soil profile with the increase of lead time. There are strong antecedent precipitation signals at the soil depths of 0.8 m when lead time is one month (Figs. 8e,g). Overall, the antecedent precipitation signals spread to the deep soil with the increase of lead time, and in middle and deep soil layers, the precipitation signals with the lead time of one month can be better stored. Moreover, the signals weaken obviously at the lead time of 2 months, especially in April–October.

Do the differences of geographical characteristics at different sites affect the relationship between ST and antecedent

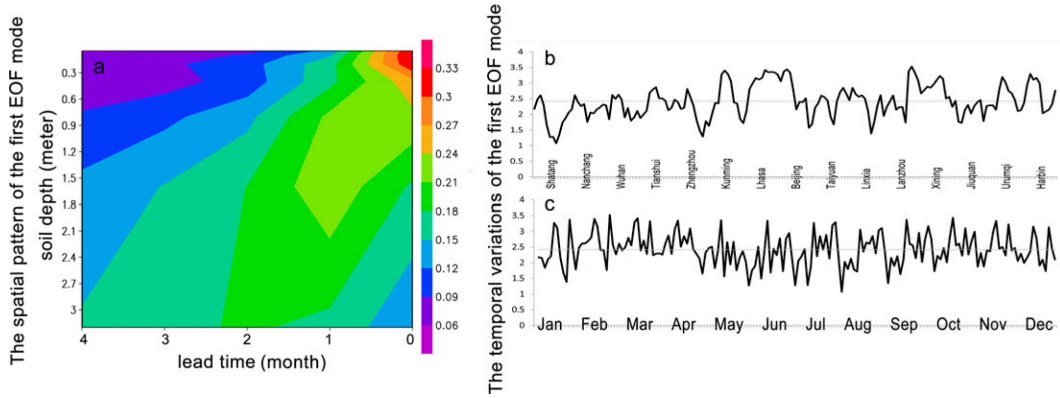

FIG. 7. The first EOF mode (explaining 87.8% variance of total variance) of correlation coefficients between ST and antecedent air temperature at different soil depths with different lead times when the month and site change. (a) The variations of EOF mode of the correlation coefficients at different soil depths with different lead time, (b) the variations of EOF mode of the correlation coefficients at different sites, and (c) the variations of EOF mode of the correlation coefficients in different months. The EOF temporal coefficients are made up of 12 months and 15 sites, (b) and (c) are obtained by adjusting the order of 12 months and 15 sites. In (b), the coefficients are arranged in the order of 15 sites, and there are 12 data points (12 months) for each site.

precipitation or air temperature? How do the effects vary significantly with soil depth and in different months? Figure 9a shows that significant linear trends in the variations of the correlation coefficients between accumulated precipitation and R-ST-T (AP-RSTT) or R-ST-P (AP-RSTP), and in the ones of the correlation coefficients between accumulated air temperature and R-ST-T (AT-RSTT) or R-ST-P (AT-RSTP) with soil depth during 1960–2013. In all soil layers, the correlation coefficients are mainly negative, except for the AP-RSTP. In other words, both R-ST-P and R-ST-T weaken with the increase of accumulated air temperature or precipitation, except for the effect of accumulated precipitation on R-ST-P in the deep soil layers (Fig. 9a). Accumulated precipitation enhances the correlations between antecedent precipitation

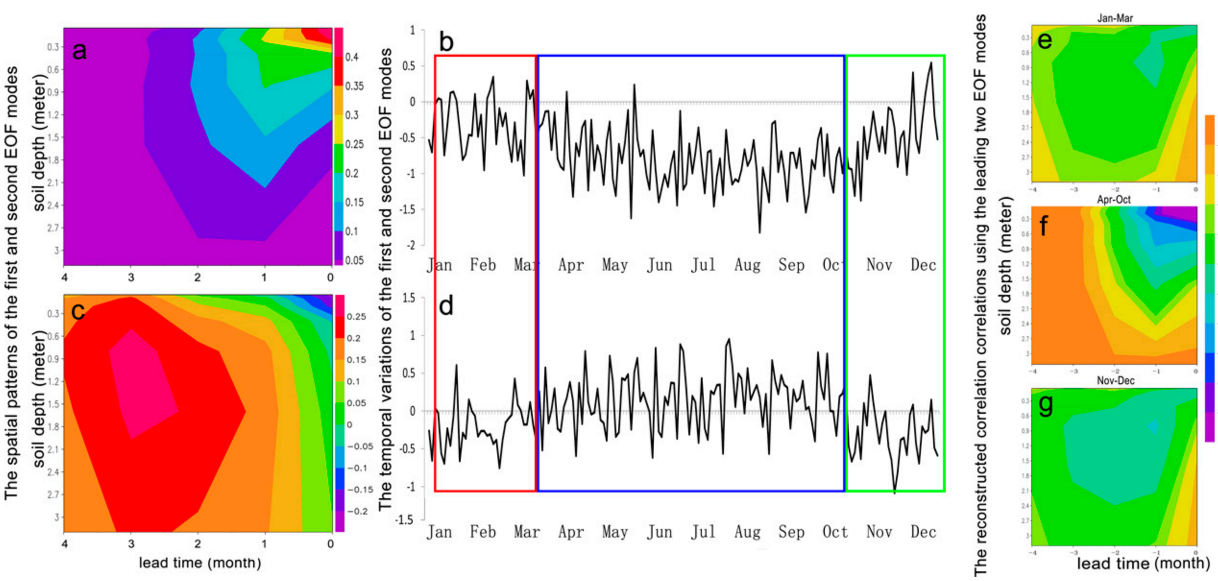

FIG. 8. The (a),(b) first and (c),(d) second leading EOF modes (explaining 32.0% and 16.8% variance of total variance, respectively) of correlation coefficients between ST and antecedent precipitation at different soil depths with different lead times when the month and site change. Panels (a) and (c) are the variations of first and second EOF modes of the correlation coefficients at different soil depths with different lead times, respectively. Panels (b) and (d) are the monthly variations of first and second EOF modes of the correlation coefficients, respectively. (e)–(g) The reconstructed total variations shown by both the first and second leading EOF modes of correlation coefficients in January–February, April–September, and November–December, corresponding to red, blue, and green panes in (b) and (d), respectively. In (b) and (d), the EOF temporal coefficients are made up of 12 months and 15 sites, and the coefficients are arranged in the order of month. There are 15 data points (15 sites) for each month in (b) and (d).

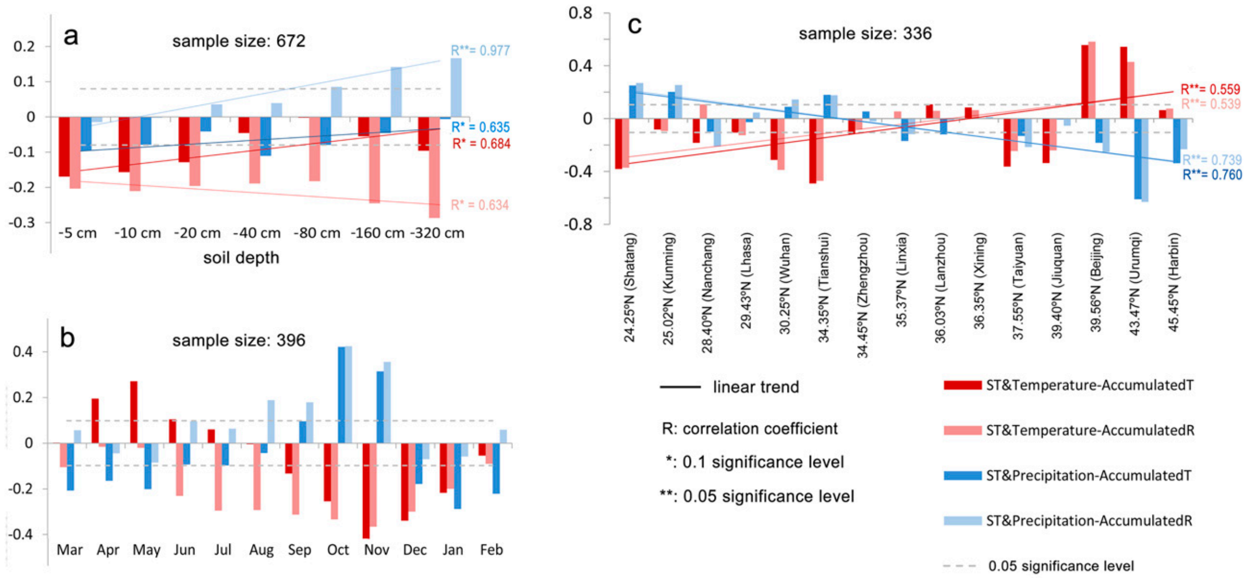

FIG. 9. The variations of correlation coefficients between accumulated temperature or accumulated precipitation and correlation coefficients between the ST and antecedent temperature (blue) or precipitation (red) with soil depth regardless of the month, site, and lead time; the oblique lines denote linear trends. ST&Temperature-AccumulatedT is the correlation coefficient between accumulated temperature and the R-ST-T (correlations between ST and antecedent temperature), and the other similar strings have similar meanings; sample size is the number of the sample for calculating ST&Temperature-AccumulatedT, etc.

and ST in the deep soil layers. Figure 9c shows that the variations of the R-ST-P and R-ST-T with latitude. As the latitude increases, the AT-RSTP and AP-RSTP change from positive to negative, while the AT-RSTT and AP-RSTT change from negative to positive. In lower latitudes, positive (negative) R-ST-T becomes much weaker (stronger) with the increase of accumulated precipitation and air temperature, this is contrary to the R-ST-P. In higher latitudes, the characteristics are opposite to those in lower latitudes. Figure 9b shows the significant monthly changes of the AP-RSTP, AP-RSTT, AT-RSTP, and AT-RSTT. From September to January in the following year, the influences of accumulated air temperature or precipitation on the R-ST-P or R-ST-T are much stronger. The AT-RSTT is negative except in April, May, and June, while the AP-RSTT is negative in all months. There are significant trends from negative to positive in AT-RSTP and AP-RSTP from December to November in the following year. In general, there are obvious linear trends with soil depths and latitudes, and significant monthly changes for the AP-RSTP, AP-RSTT, AT-RSTP, and AT-RSTT. In other

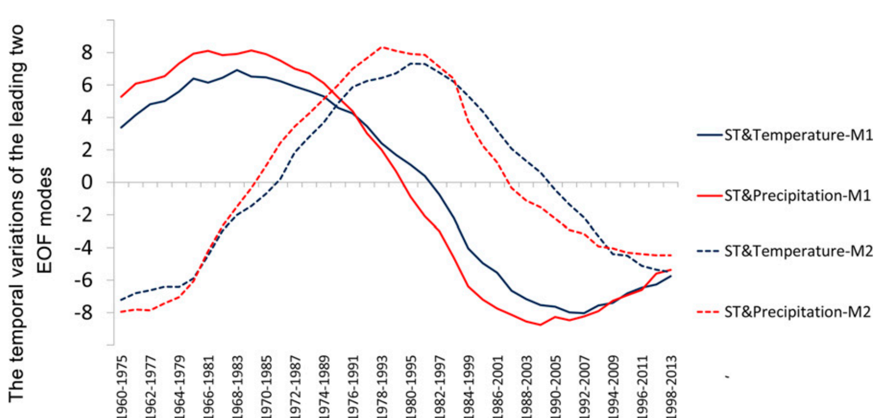

FIG. 10. The time coefficients of the first two EOF modes of the 16-yr-window sliding correlation coefficients between antecedent temperature (sold line) or precipitation (dashed line) and ST at different soil depths regardless of the month, lead time, and site. ST&Temperature denotes the correlation coefficients between ST and antecedent temperature, and ST&Precipitation has the similar meaning; M1 and M2 denote the first and second leading EOF modes, respectively.

TABLE 1. The correlation coefficients between each global climate pattern and the decadal variations of the response of ST to antecedent air temperature or precipitation. An asterisk (*) means significant at $p < 0.001$. ST&Temperature represents the sliding correlation coefficients between ST and antecedent temperature, and ST&Precipitation represents the sliding correlation coefficients between ST and antecedent precipitation. M1 and M2 represent the first and second leading EOF modes, respectively. Decadal variations of the response are represented by the temporal coefficients of the two leading EOF modes of 16-yr-window sliding correlation coefficients between ST and antecedent temperature or precipitation

	AMO	PDO	AO	IPO
ST&Temperature–M1	−0.93*	−0.21	−0.64	−0.16
ST&Temperature–M2	−0.23	0.94*	0.70*	0.93*
ST&Precipitation–M1	−0.87*	−0.27	−0.75*	−0.30
ST&Precipitation–M2	−0.30	0.91*	0.55	0.87*

words, in different soil depths, latitudes and months, the effect of accumulated precipitation or air temperature on the storage of antecedent precipitation or air temperature signals in ST are obviously different. In addition, the accumulated precipitation and accumulated air temperature show similar effect on R-ST-P and R-ST-T due to the high correlations between accumulated air temperature and accumulated precipitation (Fig. S2).

b. Decadal variations of the response of ST to antecedent precipitation or air temperature

The signals of antecedent temperature and precipitation anomalies can be stored in the ST, which is a subseasonal-to-seasonal process. Is the relationship between antecedent precipitation or temperature and ST stable on the decadal scale? If it is unstable, what are the characteristics in different decades? The sliding correlation with a 16-yr window is used to address the low-frequency variations of the correlation coefficients between ST and antecedent air temperature or precipitation, and the temporal coefficients of the two leading EOF modes of the sliding correlation coefficients shows that there are significant decadal variations with a period of more than 50 years in the relationship between ST and antecedent air temperature or precipitation. The first EOF mode leads the second one by 1/4–1/2 period, and there are similar phases between the decadal variations related to the antecedent air temperature and the ones related to the antecedent precipitation (Fig. 10).

The decadal variations in Fig. 10 exhibit the similar characteristics to some global climate patterns, such as the Atlantic multidecadal oscillation (AMO), the Pacific decadal oscillation (PDO), the Arctic Oscillation (AO), and the interdecadal Pacific oscillation (IPO). Correlation analysis shows that AMO, PDO, AO, and IPO have significant linear relationships with the decadal variations shown in Fig. 10 (Table 1). Because precipitation and air temperature are two main factors affecting ST (Helama et al. 2011), the AMO and other global patterns may affect the response of ST to antecedent meteorological conditions by changing local air temperature and precipitation. Figure 11 displays the variations of 16-yr moving average of precipitation and air temperature averaged at all sites and in all months, which correspond well to the decadal variations of the correlations between ST and antecedent precipitation or air temperature, and the correspondence is above 95% significance for air temperature or precipitation using composition analysis (Table S1). It can be

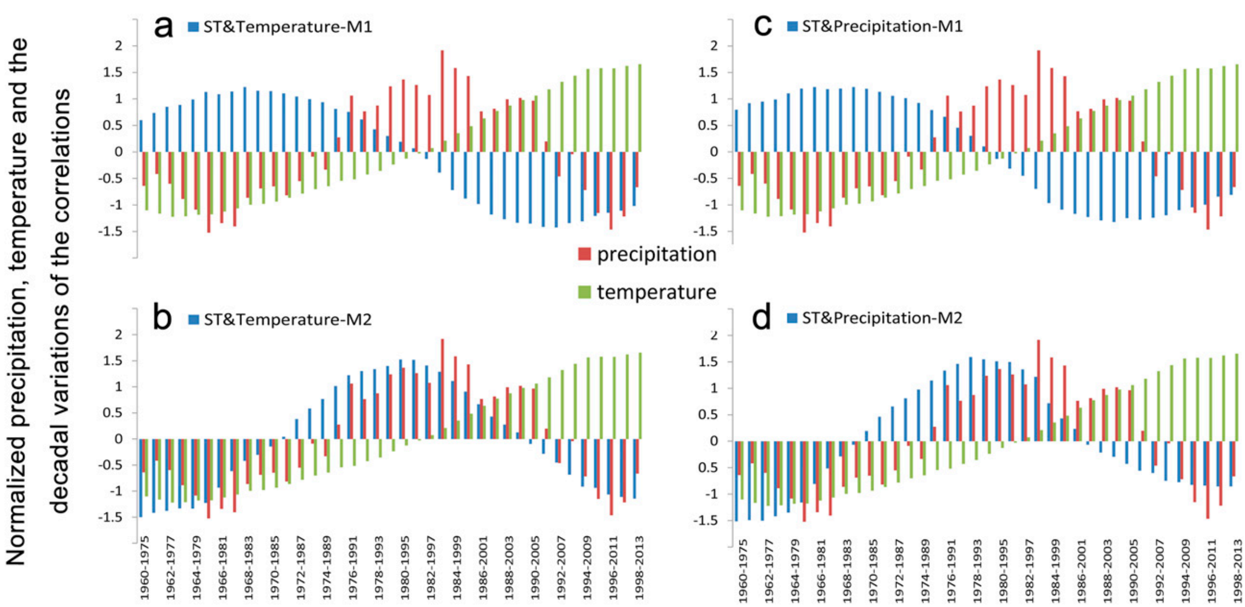

FIG. 11. Variations of 16-yr moving average of precipitation (red bar) and temperature (green bar) averaged at all sites and in all months; decadal variations of the correlations between ST and antecedent air temperature or precipitation; ST&Temperature, ST&Precipitation, M1, and M2 are the same as in Table 1.

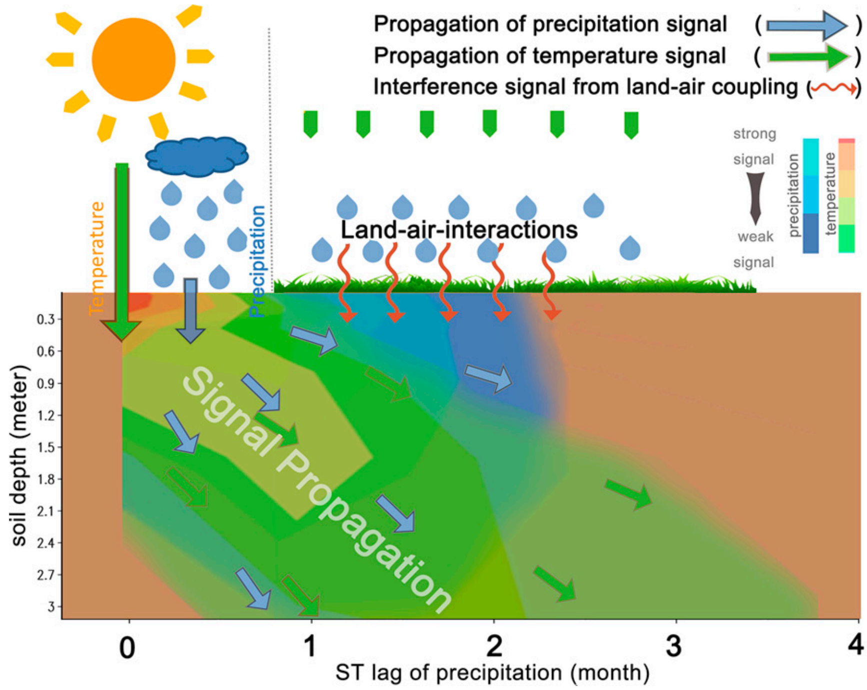

FIG. 12. Concept map for the processes of the propagation of air temperature and precipitation signals in ST, and the effect of land–air interactions on the storage of atmosphere signals in ST.

seen that the global climate patterns may affect the response of ST to antecedent precipitation and temperature by modulating the local atmospheric conditions on decadal time scale.

4. Conclusions and discussion

In the study, the storage of antecedent air temperature or precipitation signals in ST is described by lag correlation coefficients. The signals of temperature and precipitation propagate to the deep layers of soil with time. Xue et al. (2018) have demonstrated that subsurface soil temperature anomalies have important effect on the precipitation in downstream regions, so understanding the propagation of atmospheric signals to the deep soil layers is very important in improving climate prediction. The analysis based on observation shows that the storage of antecedent air temperature signals in deep ST even after four months is a widespread phenomenon in China. The antecedent air temperature signals can propagate to the soil depths of 160 and 320 cm after 1 and 2 months, respectively. The storage of antecedent air temperature signals in ST is slightly weaker during April–September, which may be related to the interference from more precipitation during growing season. There are strong correlations between precipitation and ST at the top 40-cm soil depth after one month at most sites, especially in rainy season, due to more precipitation, which shows that the storage of precipitation signals in shallow ST after one month is universal in China. As the lead time increases, antecedent precipitation signals spread to the deep soil. In April–October, the correlations are larger than the ones in January–March and November–December, implying that the response of the ST to antecedent precipitation has obvious seasonality. In middle and deep soil layers, the precipitation signals with the lead time of one month can be better stored. The stored signals rapidly weaken after 2 months, especially in April–October (Fig. 12).

It is found that the correlations between the antecedent air temperature and ST are more significant than the ones between ST and antecedent precipitation, which is consistent with previous model simulations and observations (Lin et al. 2003; Hu and Feng 2005). The changes in ST are mainly affected by air temperatures, and are modulated by precipitation (Lin et al. 2003; Qian et al. 2011). Temperature at 2 m is mainly driven by solar radiation and is mostly the superposition of several periodic signals. In precipitation, there are more high-frequency random signals, especially on daily scale. The soil is a natural filter that distinguishes the signals at different scales in the land–atmosphere interactions (She et al. 1993). Based on the analysis of the observations at the Tongyu site in China, high-frequency signals in ST are gradually filtered out as the soil depth increases (Fig. S3). Therefore, antecedent precipitation signals are much more weakly stored in middle and deep ST relative to air temperature signals.

Moreover, the R-ST-P and R-ST-T weaken with the increase of accumulated air temperature or precipitation in all soil layers, except for the effect of accumulated precipitation on R-ST-P for the deep soil layers. When the latitude increases, the AT-RSTP and AP-RSTP change from positive to negative, while the AT-RSTT and AP-RSTT change from negative to positive, this may be related to the changes in vegetation types, soil texture, etc. in different latitudes. From September to

January of the following year, the influences of accumulated air temperature or precipitation on the R-ST-P or R-ST-T are relatively stronger. In all months of a year, the increase of accumulated precipitation weakens the R-ST-T. In general, the AP-RSTP, AP-RSTT, AT-RSTP, and AT-RSTT have significant monthly changes and vary linearly with soil depth and latitude.

There are obvious decadal variations with a period of more than 50 years in the storage of antecedent air temperature or precipitation in ST, and the decadal variations may be affected by global climate patterns changing local precipitation and air temperature. The most relationships between the decadal variations of the storage and local precipitation or air temperature are within 99% significance interval based on composition analysis.

The processes of atmospheric signal propagation in ST are one of important aspects in land–atmosphere interactions. Precipitation directly changes shallow soil moisture and decreases shallow ST, which further affects deep ST. The infiltration of soil water leads to the increase of deep soil moisture. Air temperature affects shallow ST by changing sensible heat flux, affects shallow ST and soil moisture by changing ground evaporation, and changes soil moisture in the root zone by plant root uptake. The anomalies of shallow ST and moisture can cause the anomalies of deep ST and soil moisture. Under the accumulated effect of the following temperature and precipitation, the relationships between antecedent precipitation or air temperature and ST in shallow soil gradually weaken. The signals of antecedent precipitation and air temperature propagate to deep soil, gradually weaken, and spread in soil profile with time, and the weakening rate is related to the following atmospheric conditions. Moreover, soil physical properties (Ceccon et al. 2011), vegetation cover types (Zhang and Li 2018; Hu et al. 2009; Tesař et al. 2008), wind speed (Mihalakakou et al. 1997), snow (Qian et al. 2011; Iijima et al. 2010), topography changes (Wundram et al. 2010), sunshine duration (Yeşilırmak 2014), and soil freeze–thaw processes (Fang et al. 2019) can change the effect of antecedent precipitation or air temperature on ST, and have an important modulation effect on the signal propagation.

The mechanism of ST storing antecedent precipitation or air temperature signals needs further analysis by numerical sensitivity experiments. The storing and releasing of atmosphere signals in land are essential processes in land–atmosphere interactions in the climate system. Therefore, understanding the processes is of great significance in improving climate prediction and weather.

Acknowledgments. This work was supported by the National Natural Science Foundation of China (Grants 42088101, 41005047, and 41975081), the CAS "Light of West China" Program (E12903010, Y929641001), the Jiangsu University "Blue Project" outstanding young teachers training object, the Fundamental Research Funds for the Central Universities, and the Jiangsu Collaborative Innovation Center for Climate Change. We appreciate the two anonymous reviewers for the very insightful, constructive, and detailed comments to significantly improve the manuscript.

Data availability statement. The observed monthly station data in this study are provided by the China Meteorological Administration, which are available at China Meteorological Data Sharing Service System (CMDSSS) (http://data.cma.cn). The indices of AMO, PDO, AO, and Niño-3.4 are from http://www.esrl.noaa.gov/psd/data/, http://research.jisao.washington.edu/pdo/, and https://psl.noaa.gov/gcos_wgsp/. The authors declare no conflicts of interest.

REFERENCES

Beltrami, H., G. Ferguson, and R. N. Harris, 2005: Long-term tracking of climate change by underground temperatures. *Geophys. Res. Lett.*, **32**, 312–321, https://doi.org/10.1029/2005GL023714.

Ceccon, C., and Coauthors, 2011: Spatial and temporal effects of soil temperature and moisture and the relation to fine root density on root and soil respiration in a mature apple orchard. *Plant Soil*, **342**, 195–206, https://doi.org/10.1007/s11104-010-0684-8.

Chen, X., and Coauthors, 2020: The spatiotemporal variations of soil water content and soil temperature and the influences of precipitation and air temperature at the daily, monthly, and annual timescales in China. *Theor. Appl. Climatol.*, **140**, 429–451, https://doi.org/10.1007/s00704-020-03092-9.

Fan, X., 2009: Impacts of soil heating condition on precipitation simulations in the Weather Research and Forecasting model. *Mon. Wea. Rev.*, **137**, 2263–2285, https://doi.org/10.1175/2009MWR2684.1.

Fang, X., S. Luo, and S. Lyu, 2019: Observed soil temperature trends associated with climate change in the Tibetan Plateau, 1960–2014. *Theor. Appl. Climatol.*, **135**, 169–181, https://doi.org/10.1007/s00704-017-2337-9.

García-Suárez, A. M., and C. J. Butler, 2006: Soil temperatures at Armagh observatory, Northern Ireland, from 1904 to 2002. *Int. J. Climatol.*, **26**, 1075–1089, https://doi.org/10.1002/joc.1294.

Gómez, I., V. Caselles, M. J. Estrela, and R. Niclòs, 2016: Impact of initial soil temperature derived from remote sensing and numerical weather prediction datasets on the simulation of extreme heat events. *Remote Sens.*, **8**, 589, https://doi.org/10.3390/rs8070589.

Helama, S., H. Tuomenvirta, and A. Venäläinen, 2011: Boreal and subarctic soils under climatic change. *Global Planet. Change*, **79**, 37–47, https://doi.org/10.1016/j.gloplacha.2011.08.001.

Hu, H., and Coauthors, 2009: Influences of alpine ecosystem degradation on soil temperature in the freezing-thawing process on Qinghai-Tibet Plateau. *Environ. Geol.*, **57**, 1391–1397, https://doi.org/10.1007/s00254-008-1417-7.

Hu, Q., and S. Feng, 2004a: A role of the soil enthalpy in land memory. *J. Climate*, **17**, 3633–3643, https://doi.org/10.1175/1520-0442(2004)017<3633:AROTSE>2.0.CO;2.

——, and ——, 2004b: Why has the land memory changed? *J. Climate*, **17**, 3236–3243, https://doi.org/10.1175/1520-0442(2004)017<3236:WHTLMC>2.0.CO;2.

——, and ——, 2005: How have soil temperatures been affected by the surface temperature and precipitation in the Eurasian continent? *Geophys. Res. Lett.*, **32**, L14711, https://doi.org/10.1029/2005GL023469.

Iijima, Y., and Coauthors, 2010: Abrupt increases in soil temperatures following increased precipitation in a permafrost region, central Lena River basin, Russia. *Permafrost Periglacial Processes*, **21**, 30–41, https://doi.org/10.1002/ppp.662.

Kang, S., S. Kim, S. Oh, and D. Lee, 2000: Predicting spatial and temporal patterns of soil temperature based on topography, surface cover and air temperature. *For. Ecol. Manage.*, **136**, 173–184, https://doi.org/10.1016/S0378-1127(99)00290-X.

Lin, X., J. E. Smerdon, A. W. England, and H. N. Pollack, 2003: A model study of the effects of climatic precipitation changes on ground temperatures. *J. Geophys. Res.*, **108**, 4230, https://doi.org/10.1029/2002JD002878.

Liu, Y., and R. Avissar, 1999: A study of persistence in the land–atmosphere system with a fourth-order analytical model. *J. Climate*, **12**, 2154–2168, https://doi.org/10.1175/1520-0442(1999)012<2154:ASOPIT>2.0.CO;2.

Ma, Z., 1995: A preliminary analysis for the relationship between the anomalies of soil temperature and either of floods in the Yangtse–Huai river reaches and strong drought in south of Yangtse River in summer of 1991 (in Chinese). *Plateau Meteor.*, **14**, 185–190.

Mahanama, S. P. P., R. D. Koster, R. H. Reichle, and M. J. Suarez, 2008: Impact of subsurface temperature variability on surface air temperature variability: An AGCM study. *J. Hydrometeor.*, **9**, 804–815, https://doi.org/10.1175/2008JHM949.1.

Mihalakakou, G., M. Santamouris, J. O. Lewis, and D. N. Asimakopoulos, 1997: On the application of the energy balance equation to predict ground temperature profiles. *Sol. Energy*, **60**, 181–190, https://doi.org/10.1016/S0038-092X(97)00012-1.

Qian, B., E. G. Gregorich, S. Gameda, D. W. Hopkins, and X. L. Wang, 2011: Observed soil temperature trends associated with climate change in Canada. *J. Geophys. Res.*, **116**, D02106, https://doi.org/10.1029/2010JD015012.

She, J., B. Zhang, and J. Chou, 1993: The persistence and the characteristics of oscillation of soil temperatures in different depths (in Chinese). *Plateau Meteor.*, **12**, 12–17.

Tang, M., J. Wang, and J. Zhang, 1987: A primary method for predicting the spring rainfall by the winter soil temperature depth 80 cm (in Chinese). *Plateau Meteor.*, **6**, 244–255.

Tesař, M., M. Šír, M. Krejča, and J. Váchal, 2008: Influence of vegetation cover on air and soil temperatures in the Šumava Mts. (Czech Republic). *IOP Conf. Ser. Earth Environ. Sci.*, **4**, 012029, https://doi.org/10.1088/1755-1307/4/1/012029.

Wu, L., and J. Zhang, 2014: Strong subsurface soil temperature feedbacks on summer climate variability over the arid/semi-arid regions of East Asia. *Atmos. Sci. Lett.*, **15**, 307–313, https://doi.org/10.1002/asl2.504.

Wundram, D., R. Pape, and J. Löffler, 2010: Alpine soil temperature variability at multiple scales. *Arct. Antarct. Alp. Res.*, **42**, 117–128, https://doi.org/10.1657/1938-4246-42.1.117.

Xue, Y., R. Vasic, Z. Janjic, Y. M. Liu, and P. C. Chu, 2012: The impact of spring subsurface soil temperature anomaly in the western U.S. on North American summer precipitation: A case study using regional climate model downscaling. *J. Geophys. Res.*, **117**, D11103, https://doi.org/10.1029/2012JD017692.

——, and Coauthors, 2018: Spring land surface and subsurface temperature anomalies and subsequent downstream late spring–summer drought/floods in North America and East Asia. *J. Geophys. Res. Atmos.*, **123**, 5001–5019, https://doi.org/10.1029/2017JD028246.

Yang, K., and J. Zhang, 2016: Spatiotemporal characteristics of soil temperature memory in China from observation. *Theor. Appl. Climatol.*, **126**, 739–749, https://doi.org/10.1007/s00704-015-1613-9.

Yang, Y., and Coauthors, 2018: Differences of the changes in soil temperature of cold and mid-temperate zones, northeast China. *Theor. Appl. Climatol.*, **134**, 633–643, https://doi.org/10.1007/s00704-017-2297-0.

Yeşilırmak, E., 2014: Soil temperature trends in Büyük Menderes Basin, Turkey. *Meteor. Appl.*, **21**, 859–866, https://doi.org/10.1002/met.1421.

Zhang, H. X., N. M. Yuan, Z. G. Ma, and Y. Huang, 2021: Understanding the soil temperature variability at different depths: Effects of surface air temperature, snow cover, and the soil memory. *Adv. Atmos. Sci.*, **38**, 493–503, https://doi.org/10.1007/s00376-020-0074-y.

Zhang, S. Y., and X. Y. Li, 2018: Soil moisture and temperature dynamics in typical alpine ecosystems: A continuous multi-depth measurements-based analysis from the Qinghai-Tibet plateau, China. *Hydrol. Res.*, **49**, 194–209, https://doi.org/10.2166/nh.2017.215.

Zhang, T., R. G. Barry, D. Gilichinsky, S. S. Bykhovets, V. A. Sorokovikov, and J. P. Ye, 2001: An amplified signal of climatic change in soil temperatures during the last century at Irkutsk, Russia. *Climatic Change*, **49**, 41–76, https://doi.org/10.1023/A:1010790203146.